Chirality Sensing of N-Heterocycles via ^{19}F NMR

Guangxing Gu, Zhenchuang Xu, Lixian Wen, Jinhua Liang, Chenyang Wang, Xiaolong Wan, and Yanchuan Zhao*

Read Online

ACCESS | Metrics & More | Article Recommendations | SI Supporting Information

ABSTRACT: Methods to rapidly detect and differentiate chiral N-heterocyclic compounds become increasingly important owing to the widespread application of N-heterocycles in drug discovery and materials science. We herein report a ^{19}F NMR-based chemosensing approach for the prompt enantioanalysis of various N-heterocycles, where the dynamic binding between the analytes and a chiral ^{19}F-labeled palladium probe create characteristic ^{19}F NMR signals assignable to each enantiomer. The open binding site of the probe allows the effective recognition of bulky analytes that are otherwise difficult to detect. The chirality center distal to the binding site is found sufficient for the probe to discriminate the stereoconfiguration of the analyte. The utility of the method in the screening of reaction conditions for the asymmetric synthesis of lansoprazole is demonstrated.

KEYWORDS: chirality sensing, ^{19}F NMR, molecular recognition, palladium, N-heterocycles

- distal chiral center
- open binding side
- chiral *N*-heterocycles
- discrete ^{19}F signals
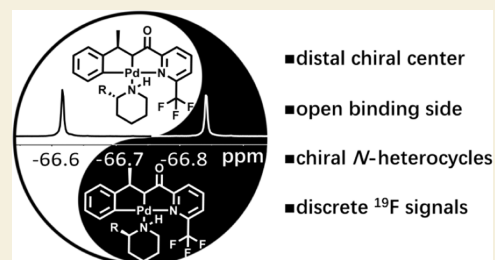
INTRODUCTION

Chiral molecules play an increasingly important role in the fields of pharmaceuticals, pesticides, and liquid crystal materials.[1−4] Synthetic methods that allow rapid access to various chiral molecules are being vigorously investigated, which greatly promotes the exploration of the unique properties of chiral substances. With the emergence of automated and high-throughput techniques, chiral molecules are now created at an unprecedented rate,[5−8] which demands innovations to solve the bottleneck in the speed of enantioanalysis. In addition to improving the pump pressure and column efficiency of chiral liquid chromatography,[9,10] in situ optical and spectroscopic methods have shown great potential in accelerating chiral analysis.[11−17] During the past decade, chemosensing systems based on fluorescence and circular dichroism have been well documented, wherein the covalent derivatization or dynamic interactions between the optical probes and analytes alter the intensity of the optical signal.[18−21] To perform the chiral analysis, these methods usually require a calibration curve constructed using enantioenriched samples with known enantiomeric excess (ee) values. Under the scenario of the development of new asymmetric reactions, access to enantiopure analytes can be challenging.

Nuclear magnetic resonance (NMR) spectroscopy is a classic method for determining optical purity, which utilizes chiral reagents to generate diastereomeric complexes of distinct spectroscopic signatures through covalent modification or transient intermolecular interactions.[22−30] In practice, its widespread adoption in chiral analysis is hampered by the complicated derivatization/purification step, the tedious signal assignments, and the overlap of NMR resonances. These

challenges are partially addressed by strategies using chiral oriented solvents, which allow NMR to probe the stereochemical information of a molecule with anisotropic NMR data.[31−34] Recently, ^{19}F NMR-based chemosensing has emerged as a burgeoning subfield in chiral analysis, where the reversible bindings between the ^{19}F-labeled probe and the target chiral analytes are transduced into simplified ^{19}F NMR signals of discrete chemical shifts.[35−39] As such, enantiomers of different configurations are simultaneously identified, allowing reliable ee determination by ratiometric analysis. This approach has been successfully applied to the chiral differentiation of diverse analytes, including primary amines, alcohols, amides, etc.[36−39] N-Heterocyclic compounds are ubiquitously found in natural products and drug molecules, exhibiting a wide spectrum of biological activities.[36] Chiral N-heterocycles are also considered privileged structural components for the exploration of transition-metal ligands and luminescent materials.[40−43] However, rapid and reliable enantioanalysis of N-heterocycles via chemosensing remains challenging. Compared to primary amines (Scheme 1a), the microenvironment around the nitrogen atom of N-heterocycles becomes more congested, which is detrimental to their affinity toward probes. Furthermore, chiral derivatization of aromatic N-heterocycles, such as pyridine, is not straightforward.
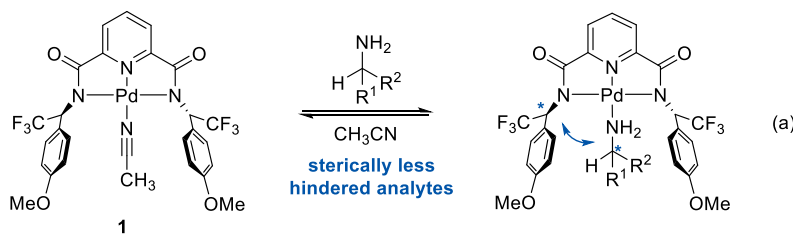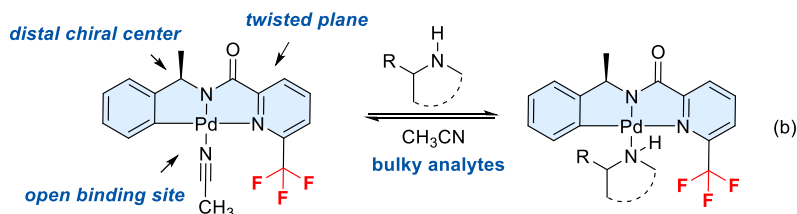
Scheme 1. Strategies for Chirality Sensing via ^{19}F NMR^a

Previous design: **confined binding pocket** and **spatially proximal chirality centers**

This work: enantiodifferentiation enabled by a distal chirality center

^{a}(a) Enantiodifferentiation using spatially proximal chirality centers. (b) Enantiodifferentiation enabled by a distal chirality center.

Scheme 2. Synthetic Route for ^{19}F-Labeled Cyclopalladium Probe 4-R
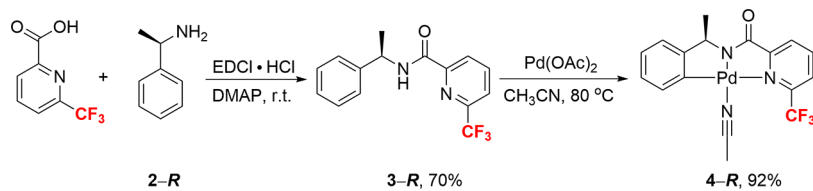
Herein, we report a ^{19}F-labeled cyclopalladium probe for the prompt chiral analysis of both aliphatic and aromatic N-heterocycles (Scheme 1b). The open binding site allows the probe to effectively recognize various sterically hindered analytes that were difficult to detect by chemosensing. A chirality center distal to the binding site is found sufficient for the probe to discern the stereoconfiguration of the analyte (Scheme 1b). The chiral information transduction strategy paves new avenues for the design of robust sensors targeting biologically relevant chiral analytes.

RESULTS AND DISCUSSION

We set out our investigation by examining the performance of previously reported ^{19}F probes in the enantiodifferentiation of N-heterocycles. Among various probes, the ^{19}F-labeled palladium pincer complexes were known to be robust for the enantioanalysis of amines (Scheme 1a).[36] Upon recognition, the analytes encapsulated in the chiral binding pocket are distinguished by the proximal ^{19}F atoms. To test whether these probes are amenable to the differentiation of N-heterocycles, we selected 1-phenyl-1,2,3,4-tetrahydroisoquinoline (A_1) as a model analyte, which is a common synthetic target for a number of asymmetric reactions.[44−47] To our surprise, no new ^{19}F NMR signal was generated when the analyte was mixed with the probe (**1**) depicted in Scheme 1a, suggesting that the chiral pocket of the pincer ligand is too confined to accommodate bulky analytes (Figure S1a−c in the Supporting Information). This observation revealed that the probe design based on spatially proximal chiral scaffolds, though powerful in promoting intimated analyte−probe interactions, is only amenable for sterically less hindered analytes. We envision that the probe with a helical-typed chirality may bind bulky analytes more effectively because the chirality can be introduced by an asymmetric twist of the probe scaffold without the need for the proximal central chirality required in previous designs (Scheme 1a). We see the monomeric cyclopalladium complexes as a promising platform to test the feasibility of our idea because they possess relatively open binding sites and are readily accessible via C−H pallada-tion.[48−50] The robustness of these complexes toward chromatographic purification implies high stability,[51] which is a desirable feature for analytical applications. By design, the central chirality at the benzylic position is envisioned to induce twisting of the square planar palladium complex (a fused 6−5−5−6 ring system, Scheme 1b), resulting in differential bindings of the chiral analytes. This intriguing signal transduction mechanism would allow the chirality of the analyte to be sensed by the trifluoromethyl moiety on the pyridine (Scheme 1b). As the chirality center is placed distal to the binding site, this probe design allows facile accommodation of bulky analytes that are otherwise difficult to enantiodifferentiate. It is noteworthy that the bridged dimers of palladium complexes were used for the chiral analysis and resolution of various amino acids; however, the complexation of monodentate N-heterocycles by these complexes is difficult.[52]

The designed probe can be readily prepared from commercially available chemicals. The condensation between 6-(trifluoromethyl)picolinic acid and (R)-1-phenylethan-1-amine (**2-R**) in the presence of EDCI·HCl produced the chiral ligand **3-R**. A subsequent C−H palladation using Pd(OAc)$_2$ in acetonitrile at 80 °C affords the desired probe
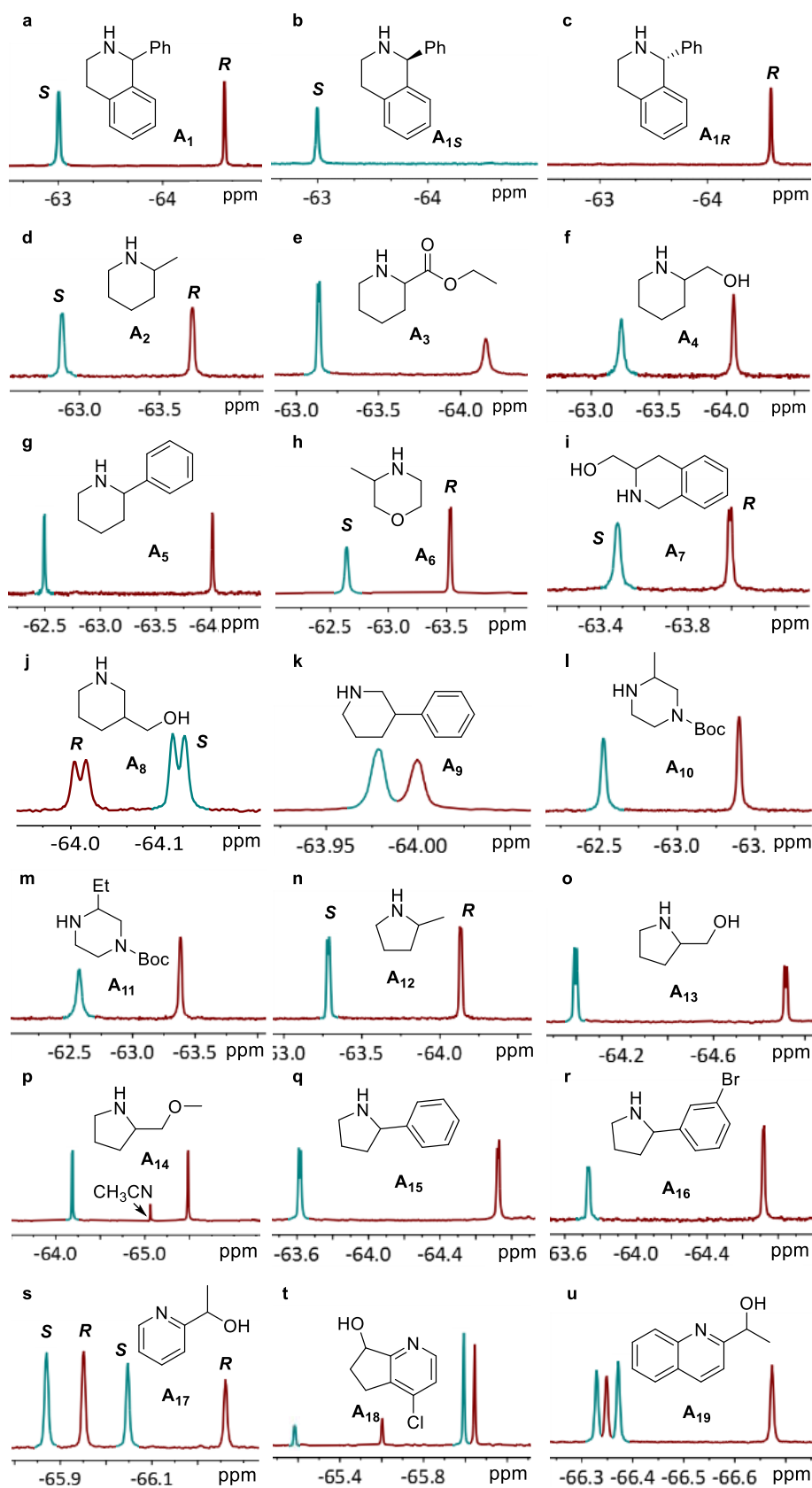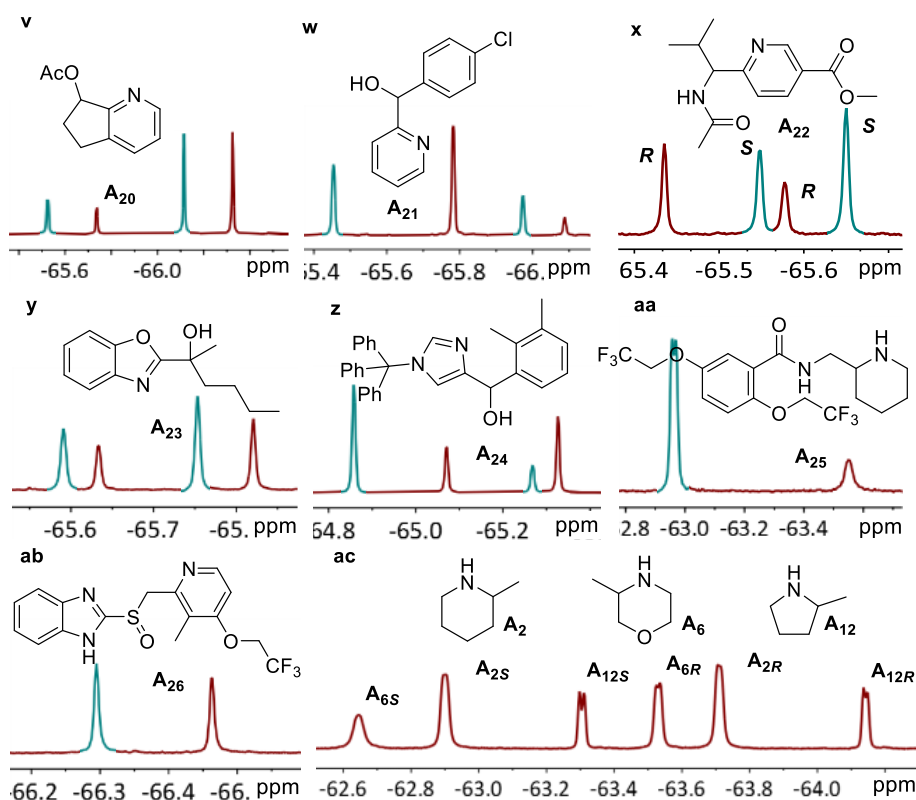
Figure 1. continued

Figure 1. (a−ac) Enantiodifferentiation of racemic N-heterocycles using probe **4-R**. (a−j, l−ac) ^{19}F NMR spectra of mixtures of **4-R** (0.9 mg) and various racemic analytes (0.5−2.0 mg) in CDCl$_3$. (k) ^{1}H-decoupled ^{19}F NMR spectra of a mixture of **4-R** (0.9 mg) and racemic **A**^{9} (1.5 mg) in CDCl$_3$. (ac) ^{19}F NMR spectrum of the probe **4-R** (ca. 3.0 mg) and 3 pairs of enantiomeric chiral N-heterocycles (each 0.5−2.0 mg) in CDCl$_3$. Note: for (a−ab), the signals in blue are produced by one enantiomer; the signals in red are produced by the other enantiomer. The absolute configuration of the analyte was assigned when the enantioenriched sample is available.

4-R in 92% yield (Scheme 2). With probe **4-R** in hand, we next evaluated its performance in the enantioanalysis of N-heterocycles by selecting a series of biologically relevant analytes. As shown in Figure 1, analyte **A**$_1$ that displays diminished affinity to the previously reported pincer-typed probe produces two well-separated ^{19}F NMR signals upon mixing with probe **4-R** in chloroform (Figure 1a), suggesting a superior recognition property of **4-R** to bind sterically bulky analytes. The ^{19}F signal appeared upfield corresponds to **A**$_1$ of the *R* configuration as confirmed by the experiments using the enantiopure analyte (Figure 1b,c). The method is amenable to the enantiodifferentiation of various 2-substituted piperidine (**A**$_2$−**A**$_5$), morpholine (**A**$_6$), and piperazine (**A**$_{10}$, **A**$_{11}$), leading to sharp and discrete ^{19}F signals. Piperidines with a substituent at 3-position are also resolvable (**A**$_8$, **A**$_9$). For these analytes, the chemical shift difference between newly generated ^{19}F signals becomes smaller as the chirality center of the analyte is too distal from that of probe **4-R**. Five-membered N-heterocycles, such as 2-substituted pyrrolidines (**A**$_{12}$−**A**$_{16}$), are easily differentiated, as evidenced by the well-separated ^{19}F signals. The linewidths of ^{19}F NMR signals produced by enantiomeric analytes are sometimes different (**A**$_3$, **A**$_{11}$), indicating that the stereoconfiguration of the analyte has an influence on the chemical exchange rate of the system. Interestingly, the splitting of the ^{19}F NMR signals is observed in the analysis of certain saturated five- and six-membered N-heterocycles (**A**$_8$, **A**$_{12}$, **A**$_{13}$, **A**$_{15}$). As ^{1}H-decoupled ^{19}F NMR experiments afford sharp singlet ^{19}F signals, the splitting is attributed to the through-space ^{1}H-^{19}F *J* coupling (Figure 2a,b). This assumption is supported by the deuteration

experiments, where a set of new singlet ^{19}F NMR signals attributed to the deuterated **A**$_{15}$ was observed (Figure 2c). This observation indicates that the current sensing scheme may also apply to the identification of the small differences between the deuterated and nondeuterated species (for more examples, see Figure S2 in the Supporting Information). We next extended our method to the enantioanalysis of aromatic N-heterocycles. Upon mixing the racemic 1-(pyridin-2-yl)-ethan-1-ol (**A**$_{17}$) with probe **4-R**, four new ^{19}F NMR signals were observed, suggesting that the binding of each enantiomer may produce two ^{19}F signals. This assumption is unambiguously confirmed by the experiment using the enantiopure analyte, where the recognition of **A**$_{17R}$ produced two ^{19}F NMR signals with chemical shifts of −65.95 and −66.26 ppm, respectively (Figure 2e). We attributed these observations to the restricted rotation of the bound analyte around the Pd−N coordination bond, which impedes the conversion between different binding models (Figure 2f). According to the density functional theory (DFT) calculation (Figures S6−S8 in Supporting Information), the energy barrier for the conversion between the complex **model-A** and **model-B** is higher than 17.4 kcal/mol, which is consistent with the slow exchange behavior on the NMR time scale. The calculation also revealed that the twisting of the planar scaffold of the probe is influenced both by the methyl-substituted chiral center and the bound analyte. Twisting angles vary between −0.11 and 15.83°, indicating that the planar scaffold of the probe is partially flexible (Figure S9 in Supporting Information). The twisting is thus adaptive to the size, shape, and stereo-configuration of the bound analyte, promoting the production
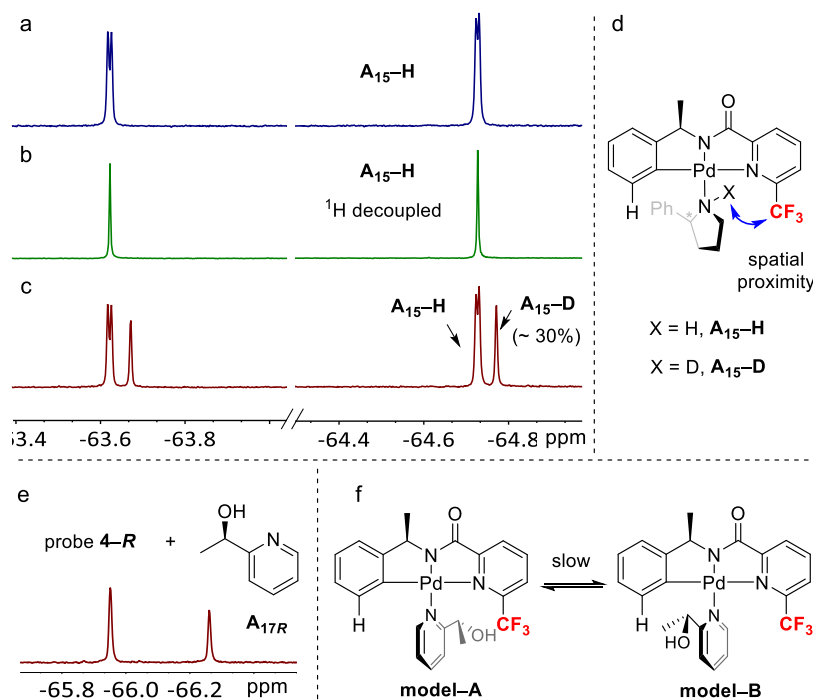
Figure 2. Investigation of binding models. (a) ^{19}F NMR spectrum of a mixture of probe **4-R** (0.9 mg) and enantiopure $\mathbf{A_{15}}$ (1.2 mg) in CDCl$_3$. (b) ^{1}H-decoupled ^{19}F NMR spectrum of a mixture of probe **4-R** (0.9 mg) and $\mathbf{A_{15}}$ (1.2 mg) in CDCl$_3$. (c) ^{19}F NMR spectrum of a mixture of probe **4-R** and partially deuterated $\mathbf{A_{15}}$ in CDCl$_3$. (d) Proposed binding models between probe **4-R** (0.9 mg) and $\mathbf{A_{15}}$ (1.2 mg). (e) ^{19}F NMR spectrum of a mixture of probe **4-R** (0.5 mg) and enantiopure (R)-1-(pyridin-2-yl)ethan-1-ol (0.4 mg) in CDCl$_3$. (f) Proposed binding models between probe **4-R** and (R)-1-(pyridin-2-yl)ethan-1-ol.

of ^{19}F NMR signals of distinct chemical shifts. ^{1}H−^{1}H nuclear Overhauser effect spectroscopy (NOSEY) experiments confirmed the spatial proximity between the probe and the bound analyte, supporting that the two ^{19}F NMR signals produced by each enantiomer correspond to different conformers of the complex (Figure S10a−c in Supporting Information). In addition to pyridines, other classes of N-heterocyclic analytes, such as quinoline ($\mathbf{A_{22}}$), benzo[d]oxazole ($\mathbf{A_{23}}$), and oxazol-5(4H)-one ($\mathbf{A_{24}}$), are also resolvable by probe **4-R**, indicating a wide analyte scope. As confirmed by the experiments using enantioenriched analytes, each enantiomer of the aromatic N-heterocycles ($\mathbf{A_{17}}$−$\mathbf{A_{24}}$) corresponds to a pair of nonadjacent ^{19}F NMR signals (Figure S3 in Supporting Information). This empirical rule may be helpful to guide the assignment of ^{19}F signals obtained in the analysis of aromatic N-heterocycles. The method is also applicable to the resolution of various heterocyclic medications, as exemplified by the analysis of flecainide ($\mathbf{A_{25}}$) and lansoprazole ($\mathbf{A_{26}}$). Given the extraordinary resolving ability of probe **4-R**, we next examine the feasibility to simultaneously detect and identify multiple chiral analytes. A series of structurally similar five- and six-membered N-heterocycles were selected to form a mixture that is difficult to resolve by traditional analytical methods. As demonstrated in Figure 1ac, the resolution of all six chiral analytes is easily achievable via our sensing scheme, highlighting the potential of this approach for the multicomponent analysis of complex real-world samples.

In chiral HPLC analysis, racemic analytes are needed in the optimization of chromatographic conditions. Without racemic standards, it is often difficult to tell whether a given sample is enantiopure. This scenario is common when analyzing natural products and certain chiral ligands, where only one enantiomer

is accessible. Our sensing scheme provides a viable solution to this unmet challenge by using a pair of enantiomeric ^{19}F probes. As depicted in Figure 3, the ^{19}F NMR signal for probe **4-R** with a bound (R)-3-methylmorpholine is the same as that for probe **4-S** with a bound (S)-3-methylmorpholine (Figure 3a,c). As such, the ^{19}F NMR spectra for the analysis of a racemic sample would be identical to that obtained by using an enantiopure analyte and both enantiomers of the ^{19}F probe (Figure 3e). To test the scope of the strategy, we next selected a series of enantiopure analytes, the enantiomers of which are either costly or inaccessible. From the comparison between the ^{19}F NMR spectra obtained using probe **4-R** and the racemic mixture of probe **4**, it is evidenced that the enantioresolution of these chiral analytes is successfully achieved (Figure 3f,g). As the binding strengths of enantiomeric analytes toward probe **4-R** are usually similar, the circumstance that only one of the enantiomers binds to the probe is unlikely.

We next tested the feasibility to use probe **4-R** to determine the ee value of enantioenriched samples. Owing to the open binding site, the affinities of probe **4-R** to enantiomeric analytes are usually similar. When the two ^{19}F NMR signals generated in the analysis of the racemic sample are of equal intensity, the enanotocomposition of the sample can be directly determined by the ^{19}F NMR integration. If there is a preference for **4-R** to bind one of the enantiomers, a correction coefficient is introduced. The use of the coefficient has been demonstrated to offset the deviation induced by the unequal affinities of enantiomeric analytes toward the chiral probe.[38,39] We next selected methylpyrrolidine ($\mathbf{A_{12}}$) and 2-(1-hydroxyethyl)pyridine ($\mathbf{A_{17}}$) as model analytes to test the performance of probe **4-R** in the enantiocomposition determination of aliphatic and aromatic N-heterocycles. As
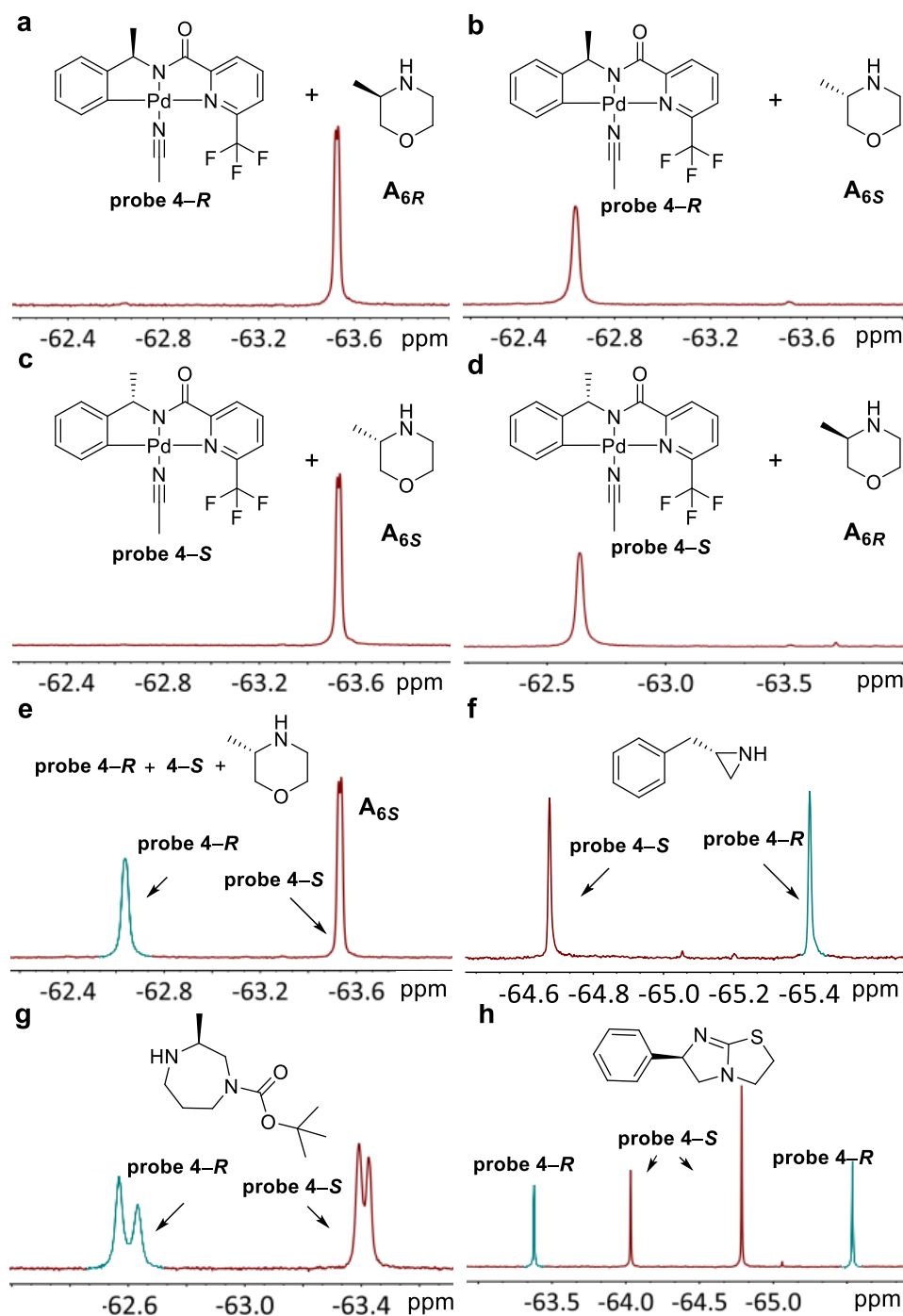
Figure 3. Enantioanalysis using only one enantiomer of the chiral analyte. (a, b) ^{19}F NMR spectra of mixtures of probe **4-R** (0.9 mg) and enantiopure (R)- or (S)-3-methylmorpholine (0.5 mg) in CDCl$_3$. (c, d) ^{19}F NMR spectra of mixtures of probe **4-S** (0.9 mg) and enantiopure (R)- or (S)-3-methylmorpholine (0.5 mg) in CDCl$_3$. (e) ^{19}F NMR spectra of mixtures of racemic probe **4** (0.9 mg) and (S)-3-methylmorpholine (0.5 mg) in CDCl$_3$. (f–h) ^{19}F NMR spectra of mixtures of racemic probe **4** (0.9 mg) and enantiopure analytes (0.4–1.2 mg) in CDCl$_3$. Note: (e–h) signals in blue−green and dark red are produced by probes **4-R** and **4-S**, respectively.

shown in Table 1, the ee values determined by our methods are all in good agreement with the actual enantiocomposition of the sample (Figures S11 and S12 in Supporting Information), with an average deviation lower than 2% (for an example in which the binding strengths of the enantiomeric analytes vary significantly, see Table S1 in Supporting Information). To further increase the accuracy of the ee assessments, quantitative NMR experiments may be applied. Our preliminary investigations indicate that the NMR

experiments with short relaxation delay (1s) give the same results as those using quantitative NMR experiments, probably due to the comparable T_1 values of ^{19}F NMR signals corresponding to the enantiomeric analytes (Figure S14 in Supporting Information). It is noteworthy that high-throughput ee value evaluation via ^{19}F NMR has been previously demonstrated, which allows the analysis of more than 1000 samples in a day using an NMR spectrometer equipped with a regular autosampler.[38]

Table 1. Evaluation of the Enantiomeric Excess Values[a]

(R)-2-methylpyrrolidine (A₁₂)				(R)-2-(1-hydroxyethyl)pyridine (A₁₇)			
actual ee (%)	calculated ee (%)[b]	corrected ee (%)[c]	deviation (%)	actual ee (%)	calculated ee (%)[b]	corrected ee (%)[c]	deviation (%)
0.00	5.7	0.0	0.0	0.0	0.0	0.0	0.0
9.6	15.3	9.7	0.1	10.5	11.9	11.9	1.4
20.1	24.0	18.5	−1.6	20.0	20.0	20.0	0.0
30.0	34.4	29.3	−0.7	29.9	30.8	30.8	0.9
39.5	43.8	39.2	−0.3	39.9	42.0	42.0	2.1
50.1	53.2	50.0	−0.1	50.2	51.0	51.0	0.8
59.5	61.8	58.1	−1.4	59.9	60.2	60.2	0.3
69.8	70.5	67.5	−2.3	69.8	68.7	68.7	−1.1
79.8	79.8	77.6	−2.2	80.0	79.1	79.1	−0.9
90.0	88.8	87.6	−2.4	89.7	87.9	87.9	−1.6

[a]NMR measurements were taken in CDCl₃ using probe 4-R (ca. 0.9 mg), 2-methylpyrrolidine (ca. 1.0 mg), and 2-(1-hydroxyethyl)pyridine (ca. 0.3 mg). [b]Calculation is based on the ¹⁹F NMR integrations associated with probe 4-R bound with R and S analytes. [c]The values are corrected based on the relative binding strength observed in the analysis of racemic samples.
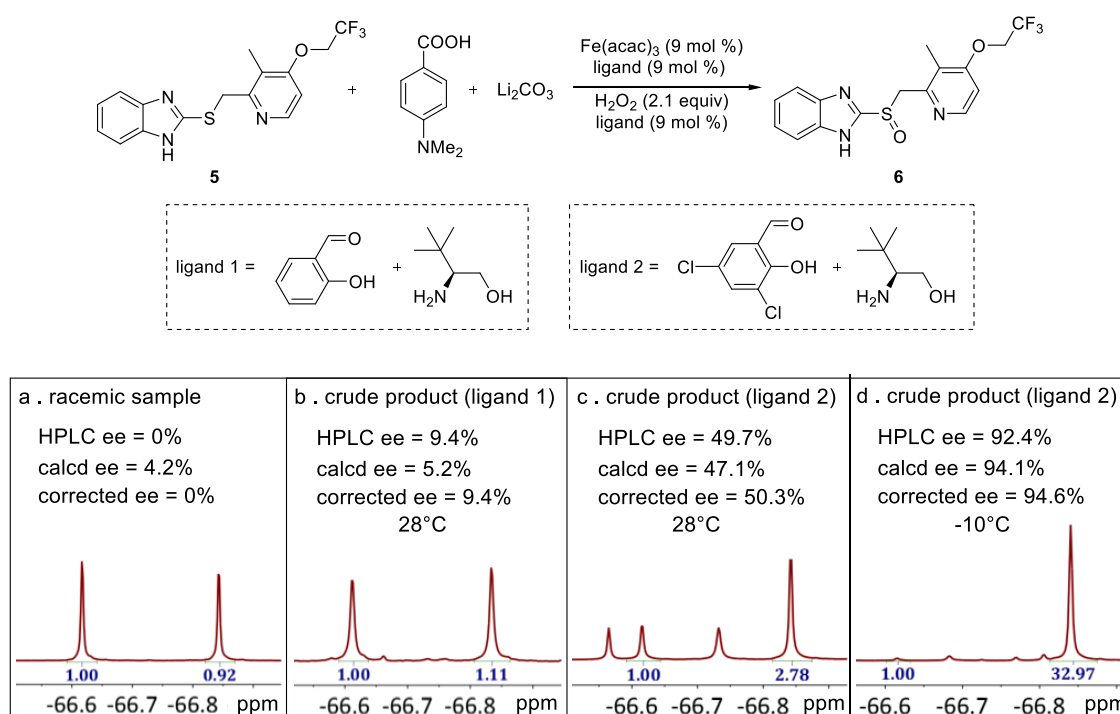

Figure 4. Evaluation of the ee values of lansoprazole produced in asymmetric oxidation using probe 4-S. (a) ¹⁹F NMR spectrum of probe 4-S (1.0 mg) and lansoprazole (ca. 1.0 mg) in acetone-d₆. (b−d) ¹⁹F NMR spectra of mixtures of probe 4-S (2.0 mg) and the crude products (ca. 2.0 mg) obtained under different conditions.

Lansoprazole is a proton pump inhibitor, which is often used to treat ulcers and other stomach problems.[53] The enantioselective synthesis of lansoprazole is of great interest because the R and S enantiomers of lansoprazole display distinct pharmacokinetics.[54] We next took the asymmetric synthesis of lansoprazole as an example to demonstrate the utility of our approach in rapid ee value assessments. In these reactions, the chiral ligand for Fe(acac)₃ is in situ formed through the condensation between (S)-2-amino-3,3-dimethyl-butan-1-ol and various salicylaldehydes, wherein enantioenriched lansoprazole is produced through the oxidation of the sulfide precursor 5 with hydrogen peroxide (Figure 4).[55] To perform the analysis, part of the reaction solution was taken and concentrated. The crude products obtained under different reaction conditions were directly mixed with the probe for ¹⁹F NMR analysis. As revealed by ¹⁹F NMR analysis (Figure 4b,c),

the substituent on the salicylaldehyde has a profound influence on the enantioselectivity of the reaction, with 3,5-dichlorosalicylaldehyde giving a much high ee (50.3%) compared to the pristine salicylaldehyde (9.4%). Lowering the reaction temperature to −10 °C significantly increases the stereoselectivity of the reaction, affording lansoprazole with an ee value of 94.6%. It is noteworthy that the remaining starting material is also observable by our method, which allows both the conversion and the enantioselectivity of the reaction to be simultaneously monitored. Furthermore, the chromatogram-like output is easily interpreted without the need for advanced spectroscopic knowledge. This appealing feature would promise the easy adoption of the ¹⁹F NMR sensing strategy in various enantioanalysis. The spectral deconvolution may further increase the accuracy of the ee evaluation when the ¹⁹F NMR signals are overlapped. A preliminary comparison

revealed that the deviations between the ee values determined by the point-to-point integration and the spectral deconvolution method are between 0.5 and 1.7% (Figure S15 in Supporting Information).

CONCLUSIONS

In summary, we have developed a new ^{19}F-labeled probe for the enantioanalysis of chiral N-heterocyclic compounds. The open binding site of the probe allows the recognition of structurally bulky analytes that are previously difficult to detect. The probe design strategy of using a distal chirality center to promote unequal twisting of the probe upon binding with a pair of enantiomeric analytes is the key to chiral discrimination. The sensing system is amenable to the screening of conditions for asymmetric reactions, visualizing both the chiral product and the prochiral substrate simultaneously. We expect that the scope of described sensing scheme can be easily extended to a wide range of analytes, providing a powerful solution to rapid and unambiguous chiral analysis.

METHODS

General Procedure for the Synthesis of Pincer Ligands

A solution of 6-trifluoromethyl-2-pyridinecarboxylic acid (500 mg, 2.62 mmol) in CH_2Cl_2 (5 mL) was added to a solution of (R)-1-phenethylamine (380 mg, 3.14 mmol), 4-dimethylaminopyridine (16 mg, 0.13 mmol), and 1-[3-(dimethylamino)propyl]-3-ethylcarbodiimide hydrochloride (598 mg, 3.14 mmol) in CH_2Cl_2 (30 mL). The reaction mixture was stirred at room temperature overnight before being quenched with water. The mixture was then extracted with EtOAc, and the organic layer was separated and washed with brine. The solution was dried over anhydrous Na_2SO_4 and concentrated under vacuum. The residue was purified by silica gel column chromatography (AcOEt/hexane = 1:4) to give ligand 3-R.

Procedure for the Preparation of ^{19}F-Labeled Probes

Ligand 3-R (200 mg, 0.68 mmol, 1.0 equiv) was added to a solution of Pd(OAc)$_2$ (167 mg, 0.75 mmol, 1.10 equiv) in acetonitrile (10 mL). The mixture was stirred at 80 °C for 12 h before cooling to room temperature. The solution was filtered through a 0.22 μm syringe filter. The filtrate was concentrated to give the crude product, which was transferred to a filter funnel and washed with water and hexane. After drying under vacuum, probe 4-R was obtained as a yellow powder.

NMR Measurements

Certain amounts of analytes were dissolved in CDCl$_3$ to obtain solutions of analytes with the required concentrations (40−100 mM). A stock solution of probe 4-R (6.8 mM, 6.0 mg in 2.0 mL of CDCl$_3$) was also prepared. Then, 300 μL of the probe solution (containing 0.9 mg of probe) and 100 μL of the analyte solution (containing 0.5−2 mg of analyte) were mixed and transferred into an NMR tube for ^{19}F NMR measurements. For Figures 1a−j,l−ac, 2e, and 3a−h, ^{19}F NMR spectra were recorded on a Bruker Avance-II 400 NMR spectrometer (376 MHz for ^{19}F nucleus) with a BBO probe at 298 K, using a default relaxation delay (D1) of 1 s and a scan number of 32. For Figures 1k, 2a−c, and 4a−d, ^{19}F NMR spectra were recorded on a Bruker Avance neo 600 NMR spectrometer (565 MHz for ^{19}F nucleus) with a BBFO probe at 298 K, using a default relaxation delay (D1) of 1 s and a scan number of 32.

ASSOCIATED CONTENT

Supporting Information

The Supporting Information is available free of charge at https://pubs.acs.org/doi/10.1021/jacsau.2c00661.

General information about materials and instruments, synthetic procedures, characterization data of products, procedures for NMR experiments, NMR spectra, DFT calculations, and HPLC traces (PDF)

AUTHOR INFORMATION

Corresponding Author

Yanchuan Zhao − *Key Laboratory of Organofluorine Chemistry, Shanghai Institute of Organic Chemistry, University of Chinese Academy of Sciences, Chinese Academy of Sciences, Shanghai 200032, China; Key Laboratory of Energy Regulation Materials, Shanghai Institute of Organic Chemistry, Chinese Academy of Sciences, Shanghai 200032, China;* orcid.org/0000-0002-2903-4218; Email: zhaoyanchuan@sioc.ac.cn

Authors

Guangxing Gu − *Key Laboratory of Organofluorine Chemistry, Shanghai Institute of Organic Chemistry, University of Chinese Academy of Sciences, Chinese Academy of Sciences, Shanghai 200032, China*

Zhenchuang Xu − *Key Laboratory of Organofluorine Chemistry, Shanghai Institute of Organic Chemistry, University of Chinese Academy of Sciences, Chinese Academy of Sciences, Shanghai 200032, China*

Lixian Wen − *Key Laboratory of Organofluorine Chemistry, Shanghai Institute of Organic Chemistry, University of Chinese Academy of Sciences, Chinese Academy of Sciences, Shanghai 200032, China*

Jinhua Liang − *Key Laboratory of Organofluorine Chemistry, Shanghai Institute of Organic Chemistry, University of Chinese Academy of Sciences, Chinese Academy of Sciences, Shanghai 200032, China*

Chenyang Wang − *Key Laboratory of Organofluorine Chemistry, Shanghai Institute of Organic Chemistry, University of Chinese Academy of Sciences, Chinese Academy of Sciences, Shanghai 200032, China*

Xiaolong Wan − *Shanghai Institute of Organic Chemistry, Chinese Academy of Sciences, Shanghai 200032, China*

Complete contact information is available at:
https://pubs.acs.org/10.1021/jacsau.2c00661

Notes

The authors declare the following competing financial interest(s): A patent has been filed on the described technique.

REFERENCES

(1) Barron, L. D. Symmetry and molecular chirality. *Chem. Soc. Rev.* **1986**, *15*, 189−223.

(2) Wang, Y.; Xu, J.; Wang, Y.; Chen, H. Emerging chirality in nanoscience. *Chem. Soc. Rev.* **2013**, *42*, 2930−2962.

(3) Kasprzyk-Hordern, B. Pharmacologically active compounds in the environment and their chirality. *Chem. Soc. Rev.* **2010**, *39*, 4466−4503.

(4) Bisoyi, H. K.; Li, Q. Liquid Crystals: Versatile Self-Organized Smart Soft Materials. *Chem. Rev.* **2022**, *122*, 4887−4926.

(5) Wang, Z.; Zhao, W.; Hao, G.; Song, B. Automated Synthesis: Current Platforms and Further Needs. *Drug Discovery Today* 2020, *25*, 2006−2011.

(6) Blair, D. J.; Chitti, S.; Trobe, M.; Kostyra, D. M.; Haley, H. M. S.; Hansen, R. L.; Ballmer, S. G.; Woods, T. J.; Wang, W.; Mubayi, V.; Schmidt, M. J.; Pipal, R. W.; Morehouse, G. F.; Ray, A. M. E. P.; Gray, D. L.; Gill, A. L.; Burke, M. D. Automated Iterative Csp³-C Bond Formation. *Nature* 2022, *604*, 92−97.

(7) Angelone, D.; Hammer, A. J. S.; Rohrbach, S.; Krambeck, S.; Granda, J. M.; Wolf, J.; Zalesskiy, S.; Chisholm, G.; Cronin, L. Convergence of Multiple Synthetic Paradigms in a Universally Programmable Chemical Synthesis Machine. *Nat. Chem.* 2021, *13*, 63−69.

(8) Collins, N.; Stout, D.; Lim, J.; Malerich, J. P.; White, J. D.; Madrid, P. B.; Latendresse, M.; Krieger, D.; Szeto, J.; Vu, V.; Rucker, K.; Deleo, M.; Gorfu, Y.; Krummenacker, M.; Hokama, L. A.; Karp, P.; Mallya, S. Fully Automated Chemical Synthesis: Toward the Universal Synthesizer. *Org. Process Res. Dev.* 2020, *24*, 2064−2077.

(9) Shen, J.; Okamoto, Y. Efficient Separation of Enantiomers Using Stereoregular Chiral Polymers. *Chem. Rev.* 2016, *116*, 1094−1138.

(10) Welch, C. J. Are We Approaching a Speed Limit for the Chromatographic Separation of Enantiomers? *ACS Cent. Sci.* 2017, *3*, 823−829.

(11) Koumarianou, G.; Wang, I.; Satterthwaite, L.; Patterson, D. Assignment-Free Chirality Detection in Unknown Samples via Microwave Three-Wave Mixing. *Commun. Chem.* 2022, *5*, No. 31.

(12) Patterson, D.; Schnell, M.; Doyle, J. M. Enantiomer-Specific Detection of Chiral Molecules via Microwave Spectroscopy. *Nature* 2013, *497*, 475−477.

(13) Zhao, Y.; Askarpour, A. N.; Sun, L.; Shi, J.; Li, X.; Alù, A. Chirality Detection of Enantiomers Using Twisted Optical Meta-materials. *Nat. Commun.* 2017, *8*, No. 14180.

(14) Warning, L. A.; Miandashti, A. R.; McCarthy, L. A.; Zhang, Q.; Landes, C. F.; Link, S. Nanophotonic Approaches for Chirality Sensing. *ACS Nano* 2021, *15*, 15538−15566.

(15) Tsukube, H.; Shinoda, S. Lanthanide Complexes in Molecular Recognition and Chirality Sensing of Biological Substrates. *Chem. Rev.* 2002, *102*, 2389−2403.

(16) Wang, L. L.; Chen, Z.; Liu, W. E.; Ke, H.; Wang, S. H.; Jiang, W. Molecular Recognition and Chirality Sensing of Epoxides in Water Using Endo-Functionalized Molecular Tubes. *J. Am. Chem. Soc.* 2017, *139*, 8436−8439.

(17) Alimohammadi, M.; Hasaninejad, A.; Luu, Q. H.; Gladysz, J. A. Λ-[Co((S,S)-Dpen)₃]³⁺2I⁻B(C₆F₅)₄⁻: A Second Generation Air- and Water-Stable Chiral Solvating Agent for Chirality Sensing (Dpen = NH₂CHPhCHPhNH₂). *J. Org. Chem.* 2020, *85*, 11250−11257.

(18) Jo, H. H.; Lin, C. Y.; Anslyn, E. V. Rapid Optical Methods for Enantiomeric Excess Analysis: From Enantioselective Indicator Displacement Assays to Exciton-Coupled Circular Dichroism. *Acc. Chem. Res.* 2014, *47*, 2212−2221.

(19) Pu, L. Fluorescence of Organic Molecules in Chiral Recognition. *Chem. Rev.* 2004, *104*, 1687−1716.

(20) Pu, L. Enantioselective Fluorescent Sensors: A Tale of BINOL. *Acc. Chem. Res.* 2012, *45*, 150−163.

(21) Wolf, C.; Bentley, K. W. Chirality Sensing Using Stereodynamic Probes with Distinct Electronic Circular Dichroism Output. *Chem. Soc. Rev.* 2013, *42*, 5408−5424.

(22) Wenzel, T. J. *Discrimination of Chiral Compounds Using NMR Spectroscopy*; Wiley: Hoboken, NJ, 2007.

(23) Hoye, T. R.; Jeffrey, C. S.; Shao, F. Mosher Ester Analysis for the Determination of Absolute Configuration of Stereogenic (Chiral) Carbinol Carbons. *Nat. Protoc.* 2007, *2*, 2451−2458.

(24) Ema, T.; Tanida, D.; Sakai, T. Versatile and Practical Macrocyclic Reagent with Multiple Hydrogen-Bonding Sites for Chiral Discrimination in NMR. *J. Am. Chem. Soc.* 2007, *129*, 10591−10596.

(25) Yang, L.; Wenzel, T.; Williamson, R. T.; Christensen, M.; Schafer, W.; Welch, C. J. Expedited Selection of NMR Chiral Solvating Agents for Determination of Enantiopurity. *ACS Cent. Sci.* 2016, *2*, 332−340.

(26) Ema, T.; Tanida, D.; Sakai, T. Versatile and Practical Macrocyclic Reagent with Multiple Hydrogen-Bonding Sites for Chiral Discrimination in NMR. *J. Am. Chem. Soc.* 2007, *129*, 10591−10596.

(27) Seo, M. S.; Kim, H. ¹H NMR Chiral Analysis of Charged Molecules via Ion Pairing with Aluminum Complexes. *J. Am. Chem. Soc.* 2015, *137*, 14190−14195.

(28) Chen, Y.-T.; Li, B.; Chen, J.-L.; Su, X.-C. Simultaneous Discrimination and Quantification of Enantiomeric Amino Acids under Physiological Conditions by Chiral ¹⁹F NMR Tag. *Anal. Chem.* 2022, *94*, 7853−7860.

(29) Seo, M. S.; Kim, H. ¹H NMR Chiral Analysis of Charged Molecules via Ion Pairing with Aluminum Complexes. *J. Am. Chem. Soc.* 2015, *137*, 14190−14195.

(30) Kuhn, L. T.; Motiram-Corral, K.; Athersuch, T. J.; Parella, T.; Pérez-Trujillo, M. Simultaneous Enantiospecific Detection of Multiple Compounds in Mixtures Using NMR Spectroscopy. *Angew. Chem., Int. Ed.* 2020, *59*, 23615−23619.

(31) Lesot, P.; Aroulanda, C.; Zimmermann, H.; Luz, Z. Enantiotopic Discrimination in the NMR Spectrum of Prochiral Solutes in Chiral Liquid Crystals. *Chem. Soc. Rev.* 2015, *44*, 2330−2375.

(32) Aroulanda, C.; Lesot, P. Molecular Enantiodiscrimination by NMR Spectroscopy in Chiral Oriented Systems: Concept, Tools, and Applications. *Chirality* 2022, *34*, 182−244.

(33) Qin, S. Y.; Jiang, Y.; Sun, H.; Liu, H.; Zhang, A. Q.; Lei, X. Measurement of Residual Dipolar Couplings of Organic Molecules in Multiple Solvent Systems Using a Liquid-Crystalline-Based Medium. *Angew. Chem.* 2020, *132*, 17245−17251.

(34) Hansmann, S.; Schmidts, V.; Thiele, C. M. Synthesis of Poly-γ-S-2-Methylbutyl-l-Glutamate and Poly-γ-S-2-Methylbutyl-d-Gluta-mate and Their Use as Enantiodiscriminating Alignment Media in NMR Spectroscopy. *Chem. - Eur. J.* 2017, *23*, 9114−9121.

(35) Xu, Z.; Liu, C.; Zhao, S.; Chen, S.; Zhao, Y. Molecular sensors for NMR-based detection. *Chem. Rev.* 2019, *119*, 195−230.

(36) Zhao, Y.; Swager, T. M. Simultaneous Chirality Sensing of Multiple Amines by ¹⁹F NMR. *J. Am. Chem. Soc.* 2015, *137*, 3221−3224.

(37) Wang, W.; Xia, X.; Bian, G.; Song, L. A Chiral Sensor for Recognition of Varied Amines Based on ¹⁹F NMR Signals of Newly Designed Rhodium Complexes. *Chem. Commun.* 2019, *55*, 6098−6101.

(38) Li, Y.; Wen, L.; Meng, H.; Lv, J.; Luo, G.; Zhao, Y. Separation-Free Enantiodifferentiation with Chromatogram-like Output. *Cell Rep. Phys. Sci.* 2020, *1*, No. 100100.

(39) Li, H.; Xu, Z.; Zhang, S.; Jia, Y.; Zhao, Y. Construction of Lewis Pairs for Optimal Enantioresolution via Recognition-Enabled "Chromatographic" ¹⁹F NMR Spectroscopy. *Anal. Chem.* 2022, *94*, 2023−2031.

(40) Taylor, A. P.; Robinson, R. P.; Fobian, Y. M.; Blakemore, D. C.; Jones, L. H.; Fadeyi, O. Modern Advances in Heterocyclic Chemistry in Drug Discovery. *Org. Biomol. Chem.* 2016, *14*, 6611−6637.

(41) Berthet, M.; Cheviet, T.; Dujardin, G.; Parrot, I.; Martinez, J. Isoxazolidine: A Privileged Scaffold for Organic and Medicinal Chemistry. *Chem. Rev.* 2016, *116*, 15235−15283.

(42) Connon, R.; Roche, B.; Rokade, B. V.; Guiry, P. J. Further Developments and Applications of Oxazoline-Containing Ligands in Asymmetric Catalysis. *Chem. Rev.* 2021, *121*, 6373−6521.

(43) Chen, D.; Su, S. J.; Cao, Y. Nitrogen Heterocycle-Containing Materials for Highly Efficient Phosphorescent OLEDs with Low Operating Voltage. *J. Mater. Chem. C* 2014, *2*, 9565−9578.

(44) Ji, Y.; Shi, L.; Chen, M. W.; Feng, G. S.; Zhou, Y. G. Concise Redox Deracemization of Secondary and Tertiary Amines with a Tetrahydroisoquinoline Core via a Nonenzymatic Process. *J. Am. Chem. Soc.* 2015, *137*, 10496−10499.

(45) Chang, M.; Li, W.; Zhang, X. A Highly Efficient and Enantioselective Access to Tetrahydroisoquinoline Alkaloids: Asym-

metric Hydrogenation with an Iridium Catalyst. *Angew. Chem.* **2011**, *45*, 10867−10869.

(46) Zhu, J.; Tan, H.; Yang, L.; Dai, Z.; Zhu, L.; Ma, H.; Deng, Z.; Tian, Z.; Qu, X. Enantioselective Synthesis of 1-Aryl-Substituted Tetrahydroisoquinolines Employing Imine Reductase. *ACS Catal.* **2017**, *7*, 7003−7007.

(47) Barrios-Rivera, J.; Xu, Y.; Wills, M. Asymmetric Transfer Hydrogenation of Unhindered and Non-Electron-Rich 1-Aryl Dihydroisoquinolines with High Enantioselectivity. *Org. Lett.* **2020**, *22*, 6283−6287.

(48) He, G.; Lu, G.; Guo, Z.; Liu, P.; Chen, G. Benzazetidine Synthesis via Palladium-Catalysed Intramolecular C-H Amination. *Nat. Chem.* **2016**, *8*, 1131−1136.

(49) Zang, Z. L.; Karnakanti, S.; Zhao, S.; Hu, P.; Wang, Z.; Shao, P. L.; He, Y. Synthesis of Spiro-Dihydroquinoline and Octahydrophenanthrene Derivatives via Palladium-Catalyzed Intramolecular Oxidative Arylation. *Org. Lett.* **2017**, *19*, 1354−1357.

(50) Usui, K.; Haines, B. E.; Musaev, D. G.; Sarpong, R. Understanding Regiodivergence in a Pd(II)-Mediated Site-Selective C-H Alkynylation. *ACS Catal.* **2018**, *8*, 4516−4527.

(51) Yang, Q. L.; Wang, X. Y.; Wang, T. L.; Yang, X.; Liu, D.; Tong, X.; Wu, X. Y.; Mei, T. S. Palladium-Catalyzed Electrochemical C-H Bromination Using NH_4Br as the Brominating Reagent. *Org. Lett.* **2019**, *21*, 2645−2649.

(52) Böhm, A.; Seebach, D. Determination of Enantiomer Purity of *β*- and *γ*-Amino Acids by NMR Analysis of Diastereoisomeric Palladium Complexes. *Helv. Chim. Acta* **2000**, *83*, 3262−3278.

(53) Lai, K. C.; Lam, S. K.; Chu, K. M.; Wong, B. C. Y.; Hui, W. M.; Hu, W. H. C.; Lau, G. K. K.; Wong, W. M.; Yuen, M. F.; Chan, A. O. O.; Lai, C. L.; Wong, J. Lansoprazole for the Prevention of Recurrences of Ulcer Complications from Long-Term Low-Dose Aspirin Use. *N. Engl. J. Med.* **2002**, *346*, 2033−2038.

(54) Katsuki, H.; Yagi, H.; Arimori, K.; Nakamura, C.; Nakano, M.; Katafuchi, S.; Fujioka, Y.; Fujiyama, S. Determination of R(+)- and S(-)-lansoprazole using chiral stationary-phase liquid chromatography and their enantioselective pharmacokinetics in humans. *Pharm. Res.* **1996**, *13*, 611−615.

(55) Nishiguchi, S.; Izumi, T.; Kouno, T.; Sukegawa, J.; Ilies, L.; Nakamura, E. Synthesis of Esomeprazole and Related Proton Pump Inhibitors through Iron-Catalyzed Enantioselective Sulfoxidation. *ACS Catal.* **2018**, *8*, 9738−9743.